Indian Journal of Chemistry
Vol. 60A, December 2021, pp. 1551-1556

New Mn(II)-coordination polymer based on flexible benzimidazol ligand: Crystal structure and application on osteosarcoma

Zhiming Ni[§], Shuchen Ding[§], Yuan Qu, Hongbo Yu & Junjie Xia*

Department of Orthopedic, The 903th Hospital of Joint Logistics Support Force of the Chinese People's Liberation Army, Hangzhou 310004, China

*E-mail: xia_1172021@163.com

Received 04 September 2021; revised and accepted 24 November 2021

In this study, a Mn(II)-based coordination polymer with the chemical composition of $\{[Mn(L)(TBTA)(H_2O)_2]\cdot H_2O\}_n$ (**1**) has been prepared by reacting $Mn(OAc)_2\cdot 2H_2O$ with the flexible ligand 1,4-bis(5,6-dimethylbenzimidazol-1-yl)-2-butylene in the aid of the carboxylic acid ligand tetrabromoterephthalic acid (H_2TBTA) through the mixed-ligand method. Its application value on osteosarcoma has been measured, and the internal principle is discussed simultaneously. The inhibitory activity of the new compound on the multiplication of osteosarcoma cells is evaluated using the Cell Counting Kit-8 detection kit. The facilitation of the LKB1-mTORC1 signalling pathway is estimated via real-time RT-PCR.

Keywords: Coordination polymer, Osteosarcoma, RT-PCR

Osteosarcoma is a familiar tumor, and 90% of juvenile metastases occur in primary lung malignant bone tumors. Although the survival time of patients with osteosarcoma combined with standard chemotherapy and limb-saving surgery is longer than before, the prognosis of patients with lung metastases remains poor with the improvement of treatment effect[1]. Bone metastasis accounts for 15%–20% of metastatic tumors in the body, which is lower than the incidence rates of liver and lung metastases. Malignant tumors in the lung, prostate, and thyroid are the most familiar primary tumors, taking up approximately 80% of whole cases[2,3]. Thus, understanding the principle of bone metastasis is important to improve the prevention and cure of bone metastasis.

Nowadays, metal complexes based on benzimidazole derivatives with diversified structure, including cyclic complexes, have attracted increasing attention[4]. Benzimidazole derivatives have diverse coordination functions that benefit this type of metal organic structure[5-7]. Metal complexes based on benzimidazole have also attracted wide publicity because of their outstanding properties and wide applications in various industries, such as supramolecular chemistry, catalysis, luminescence, and pharmacology[8-11]. Benzimidazole has a double ring structure formed by the combination of imidazole and benzene. It is used in the research and development of new drugs. Many compounds including this motif were clinically admitted for application as anti-helminth drugs (such as thiabendazole), proton pump inhibitors (such as lansoprazole), antiviral drugs (such as enviradine), and antihypertensive drugs (such as telmisartan)[12-15]. In addition to the above concerned medicinal functions, benzimidazole complexes also possess antitumor and other related bioactivities[16,17]. On the other hand, Manganese(II) ion is the required co-factor in many ubiquitous enzymes. Research has proved that Mn(II) ion is mainly uptaken and transported by divalent metal transporter (DMT-1) and transferrin receptor (TfR), which is high expressed in some tumor tissues[18,19]. Transporting mechanism of Mn(II) *in vivo* makes Mn(II)-based compounds possible to be tumor-targeted. Biochemically active Mn(III)-salen and Mn(III)-salphen compounds were reported to induce nuclear fragmentation and apoptosis of HeLa cells[20]. Chen and co-workers reported that Mn(II) compounds with N-substituted di(picolyl)amine inhibits the proliferation of human glioma cells (U251) and HepG-2 cells *in vitro*[21].

In the present study, an innovative Mn(II)-based coordination polymer (CP) with the technical term of $\{[Mn(L)(TBTA)(H_2O)_2]\cdot H_2O\}_n$ (**1**) was prepared by reacting $Mn(OAc)_2\cdot 2H_2O$ with the flexible ligand 1,4-bis(5,6-dimethylbenzimidazol-1-yl)-2-butylene in the aid of the carboxylic acid ligand

§These authors contributed equally to this work

tetrabromoterephthalic acid (H_2TBTA) through the mixed-ligand method. The prepared coordination polymer **1** was structurally discussed with single crystal X-ray diffraction and was further detected by infrared (IR) spectroscopy, powder X-ray diffraction (PXRD), elemental analyses, and thermogravimetric analysis (TGA). Serial biological experimentations were performed to measure the therapeutic effect of the new compound against osteosarcoma.

Materials and Methods

All reagents were analytical grade and used as received without further purification. Carbon, hydrogen, and nitrogen were analyzed using the Perkin-Elmer model 240C analyzer. The IR spectrum on the Nicolet spectrometer with KBr pellets was recorded at 400–4000 cm^{-1}. The PXRD pattern was obtained using the Bruker D8 Advance X-ray diffractometer applying Cu-*Kα* radiation (0.15418 nm) at 40 kV and 30 mA. TGA results were implemented via the Perkin Elmer thermogravimetric analyzer from roomtemperature to 700 °C with a heating rate of 20 K min^{-1} under nitrogen environment.

Preparation and characterization for {[Mn(L) (TBTA) $(H_2O)_2$]·H_2O}$_n$ (1)

In a 25 mL Teflon-lined high pressure vessel, 10 mL of H_2O, 53 mg of $Mn(OAc)_2·2H_2O$, and 48.1 mg of 34.4 mg L^{-1} H_2TBTA were mixed to obtain the compound. Then, it was stored at 140 °C for 72 h. After lowering to the normal environment at a speed of 10 °C·h^{-1}, pink crystals were produced by filtration and washing. The yield was 37.2%. Anal. Calcd. (%) for **1**($C_{30}H_{30}Br_4MnN_4O_7$): C, 38.61; H, 3.24; N, 6.00. Found (%): C, 38.53; H, 3.79; N, 5.82. IR (KBr, cm^{-1}, Fig S1): 3567 m, 1577 s, 1506 s, 1407 m, 1326 s, 1301 m, 1212w, 1081w, 960w, 872 m.

XRD data were obtained using the Oxford Xcalibur E diffractometer. Statistical analysis of diverse intensity data was recorded via CrysAlisPro software, and the result was converted into HKL format. The pattern of SHELXS applying the direct method was used to form the fundamental structure, and the pattern of SHELXL-2014 applying the least square method was modified. Various inhomogeneous parameters were employed to refine non-H atoms. The whole H atoms adopting AFIX program were linked with the C atom. Table 1 reveals the particular data of complex **1**.

Cell Counting Kit-8 detection kit

The inhibitory effect of the new compound on the multiplication of osteosarcoma cells was estimated using the Cell Counting Kit-8 assay in accordance with the manufacturer's instructions with some modifications. In brief, OUMS-27 osteosarcoma cells in the logical growth period were gathered and inoculated into 96-well plates with the ultimate fate of 10^4 cells / well. The cells were set in an incubator at 37 °C and 5% CO_2. After half a day of cultivation, the new compound was incubated at a continuous concentration (0–80 μM). The cell culture medium was abandoned, and a new medium containing CCK-8 reagent was poured in the well. After the specified treatment, the absorbance of every well was estimated at 490 mm. The whole experimental procedure was repeated three times, and the data are expressed as mean ± SD.

Table 1 — Experimental details and crystallographic results of compound **1**

Empirical formula	$C_{30}H_{28.67}Br_4MnN_4O_{6.67}$
Formula weight	926.50
Temperature (K)	296.15
Crystal system	monoclinic
Space group	C2/c
a (Å)	9.3261(12)
b (Å)	19.246(2)
c (Å)	18.672(5)
α (°)	90
β (°)	101.026(2)
γ (°)	90
Volume ($Å^3$)	3289.5(10)
Z	4
ρ_{calc} (g/cm^3)	1.871
μ (mm^{-1})	5.311
Reflections collected	10145
Independent reflections	3884 [R_{int} = 0.0374, R_{sigma} = 0.0510]
Data/restraints/parameters	3884/43/238
Goodness-of-fit on F^2	1.072
Final R indexes [I>=2σ (I)]	R_1 = 0.0424, ωR_2 = 0.1045
Final R indexes [all data]	R_1 = 0.0733, ωR_2 = 0.1155
Largest diff. peak/hole (e $Å^{-3}$)	0.78/-0.97
CCDC	2104612

Real-time RT-PCR

The activity of the LKB1-mTORC1 signalling pathway in osteosarcoma cells after using the compound was detected by real-time RT-PCR. The work was performed following the instructions. OUMS-27 osteosarcoma cells in the logical growth period were gathered and inoculated into six-well plates with an ultimate fate of 10^6 cells per well. The cells were cultured in an incubator at 37 °C and 5% CO_2 for half a day and then fresh compounds were injected to the indicated concentration for treatment.

RNA was extracted using TRIZOL reagent. After estimating the RNA concentration, it was reverse transcribed into cDNA. The relative expression of mTORC1 and LKB1 was detected by real-time RT-PCR, and *gapdh* was treated as the internal control.

Results and Discussion

Structural characterization

The results of single crystal analysis and structural decomposition gathered at normal temperature explain that complex **1** forms the crystal in monoclinic space group *C*2/*c*, and the asymmetric part concludes half a Mn(L)(TBA) entity, a coordinated water molecule, and half a non-coordinated water molecule, as shown in Fig. 1a. The Mn(II) centrum explains the 6-coordination with N1A and N1 atoms (symmetry code is A = $-x$, y, $-z + 1/2$) from double various nitrogen-containing ligands, O1A and O1 atoms from double various fully deprotonated $TBTA^{2-}$ ligands, and double coordinated water molecules (O1WA, O1W). These components produce a crooked octahedral structure. The bond angle around the Mn(II) centrum ranges from 86.62(2)° to 178.57(1)°, and the Mn–O/N bond distances are in the range of 2.063(2)–2.133(3) Å. The Mn–O/N bond distances are comparable with those observed in other Mn(II)-based coordination polymers constructed from the carboxylic acid and N-donor co-ligands such as $\{[Mn(dpb)(4,4'\text{-bibp})]\cdot H_2O\}_n$ (Mn–O/N: 2.087(8)-2.218(5) Å) and $[Mn_{0.5}(PHDI)_{0.5}(DHTA)_{0.5}]_n$ (Mn–O/N: 2.016-2.136 Å) [22, 23]. In compound **1**, the L ligand takes the trans conformation. The torsion angle of $N_{donor}\cdots N\text{–}C_{sp3}\cdots C_{sp3}$ is 56.06(4)°, and the dihedral angle between the planes of the adjacent benzimidazole rings in the L ligand is 49.33(1)°. L shows as a μ_2-ligand, linking with neighbouring metal centers to construct a rectilinear 1D $[Mn(L)]_n$ chain (Fig. 1b). The $TBTA^{2-}$ ligands show as $(\kappa^1\text{-}\kappa^0)\text{-}(\kappa^1\text{-}\kappa^0)\text{-}\mu_2$to prolong the 1D $[Mn(L)]_n$ chain into a 2D lamina by linking with the Mn(II) centers (Fig. 1c). The 2D layer can be used as a 4-connection **sql** network via the point symbol $(4^4\cdot6^2)$ (Fig. 1d).

PXRD detections were conducted for these compounds to estimate the phase purity of the compounds (Fig. 2a). The apex of the study and simulated PXRD pictures are consistent with one

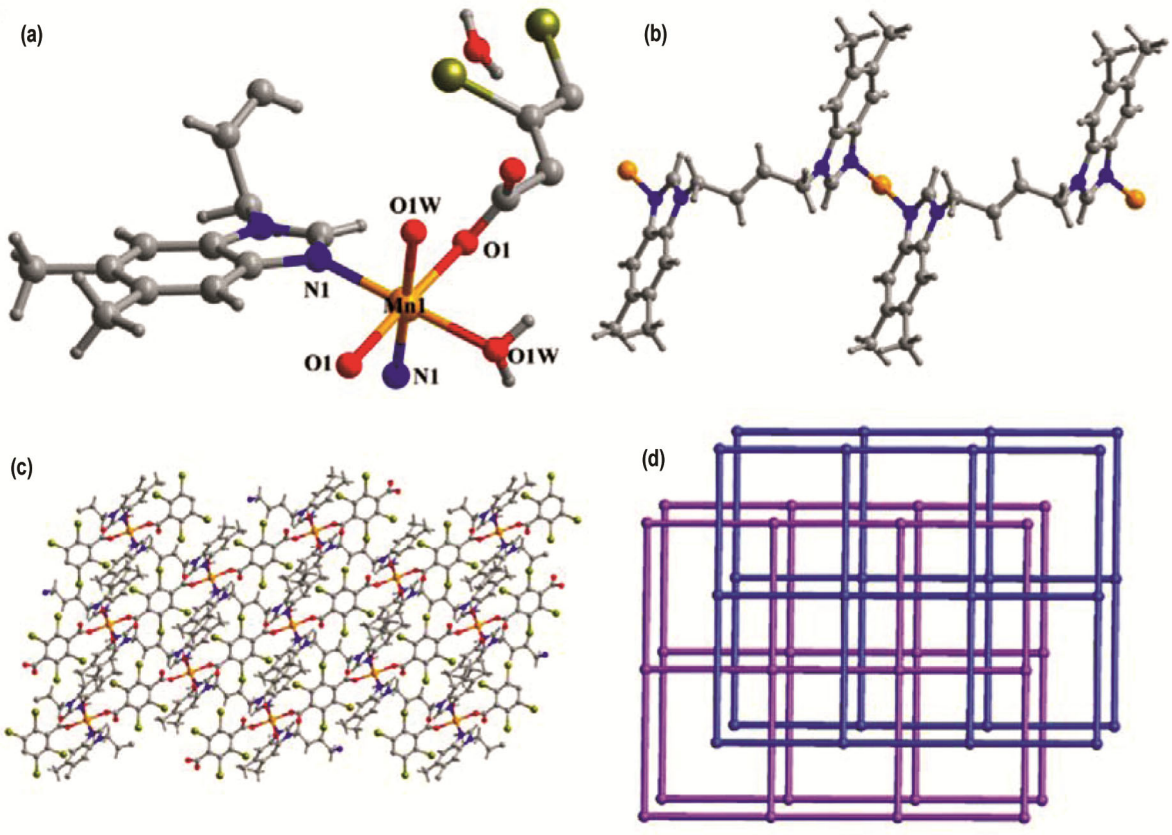

Fig. 1 — (a) Least building part, (b) one-dimensional Mn-L chain, (c) 2D framework and (d) four-connection **sql** net of **1**

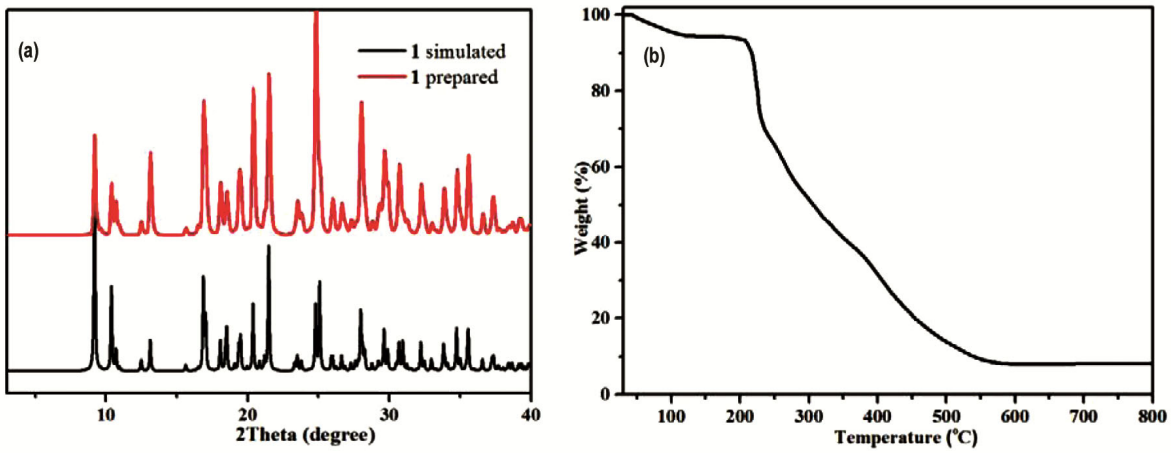

Fig. 2 — (a) PXRD patterns and (b) TGA curve of compound **1**

another, illustrating that the crystal framework is authentically a delegate of the blocky crystal compounds. The difference in strength may be due to the quality of the crystal sample. To understand thermal decomposition, TGA studies of compound **1** were conducted at the temperature range of 25 °C–800 °C under the condition of N_2 atmosphere at a heating speed of 10 °C min^{-1} (Fig. 2b). The TGA curve of **1** shows that the weight loss is 5.62% in the range of 40 °C–120 °C, which is consistent with the subtraction of water molecules (calcd 5.79%). The second weight subtraction (86.72%) is in the range of 190 °C–578 °C. One reason for weight loss is the decomposition of $TBTA^{2-}$and L ligands. The final product above the temperature of 600 °C might be ascribed to MnO (observed: 7.83%, calcd: 7.51%).

In the IR spectra of **1**, there is an absorption peak around 3400 cm^{-1}, indicating the existence of water molecules. No obvious peak is observed around 1700 cm^{-1}, illustrating that the H_2TBTA ligands are all completely deprotonated. The characteristic peak of 1577 cm^{-1} for **1** could be attributed to the asymmetric (ν_{as}(COO)) vibrations. The peak at 1326 cm^{-1} is derived from symmetric (ν_s(COO)) vibrations. The separations between the characteristic peaks ($\Delta\nu$=[ν_{as}(COO)–ν_s(COO)]) for demonstrate that the $TBTA^{2-}$ ligands have the monodentate coordination mode ($\Delta\nu$=251 cm^{-1} for **1**). The broad band of **1** at 1506 cm^{-1} result from the $\nu_{C=N}$ stretching of the benzimidazole-based ligands. In order to research of the luminescence properties of **1**, the solid-state luminescence spectra of ligand L and **1** were investigated at room temperature (Fig. S2, Supplementary Data). The free L ligand displays the emission maxima at 319 nm and the excitation maxima at 298 nm, which can be attributed to $\pi^*\rightarrow\pi$ transitions.

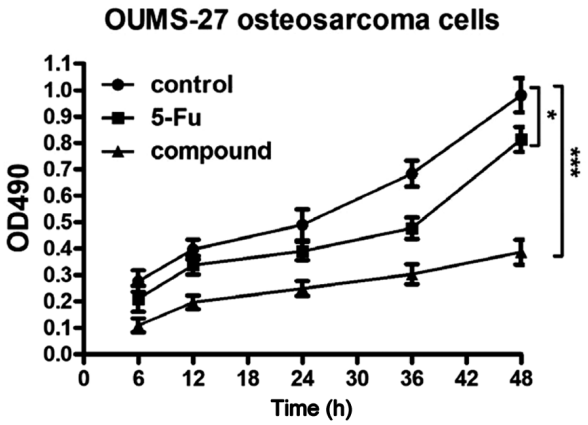

Fig. 3 — Treatment activation on the proliferation of OUMS-27 osteosarcoma cells

Compound **1** emits strong luminescence with maxima peaks at 312 nm (λ_{ex} = 279 nm). In comparison with ligand L, the emission maxima of **1** has slight blue-shifted of 7 nm. The strong luminescence emission of compound **1** may due to the ligand-to-ligand charge transfer because their similar profiles.

Inhibition of the new compound on the proliferation of OUMS-27 osteosarcoma cells

After the design and formation of the new compound with fresh structure, its treatment activation on the proliferation of OUMS-27 osteosarcoma cells was determined. OUMS-27 osteosarcoma cells in the logical growth period accumulated and fostered into the cell culture plate, and then the compound was injected at continuous different dilutions. The proliferation of metastatic bone cancer cells was evaluated via CCK-8 assay. As shown in Fig. 3, the proliferation of OUMS-27 osteosarcoma cells in the control model was high. After using the fresh compound, the proliferation of OUMS-

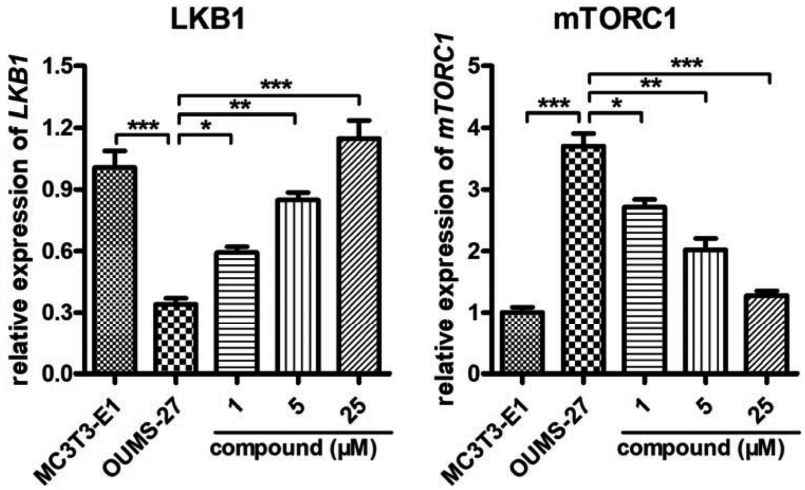

Fig. 4 — Activation of the LKB1-mTORC1 signaling pathway in osteosarcoma cells

27 osteosarcoma cells significantly reduced, which is tremendously unequal from the control model. The inhibition of the new compound was much stronger than the positive control medicine 5-Fu.

Regulated LKB1-mTORC1 signalling pathway activation in osteosarcoma cells

The compound showed excellent regulatory influence on the LKB1-mTORC1 signalling pathway in osteosarcoma cells. OUMS-27 osteosarcoma cells in the logical growth period were accumulated and fostered into the cell culture medium, and then the compound was injected at indicated various concentrations. Real-time RT-PCR was recommended to evaluate the activation of the LKB1-mTORC1 signalling pathway in the osteosarcoma cells. The new compound showed great inhibitory activation on the proliferation of the osteosarcoma cells. As previously reported, the LKB1-mTORC1 signalling pathway shows a vital part in the development of osteosarcoma development. Thus, real-time RT-PCR was further implemented, and the activity of the LKB1-mTORC1 signalling pathway was evaluated. As shown in Fig. 4, the level of LKB1 tremendously reduced and the level of mTORC1 decreased in the osteosarcoma cells in contrast to the control group. Obvious diversity occurred between two groups. Under the injection of the fresh compound, the relative expression of LKB1 was regulated and the mTORC1 level significantly reduced. The biological activity of the fresh compound was dose dependent.

Conclusions

We prepared Mn(II)-based coordination polymer by reacting $Mn(OAc)_2 \cdot 2H_2O$ with the flexible ligand 1,4-bis(5,6-dimethylbenzimidazol-1-yl)-2-butylene in the aid of the carboxylic acid ligand tetrabromoterephthalic acid. The prepared coordination polymer **1** was structurally discussed via single-crystal XRD and was further detected by IR spectral, EA, PXRD, and TG analyses. The cell counting Kit-8 detection kit revealed that the compound could tremendously lower the proliferation of the osteosarcoma cells. Moreover, the activity of the LKB1-mTORC1 signalling pathway in the osteosarcoma cells was inhibited by the new compound in a dose-dependent manner. The compound could be an extraordinary candidate for osteosarcoma therapy by inhibiting the proliferation of osteosarcoma cells and activity of the LKB1-mTORC1 signaling pathway in the osteosarcoma cells.

Supplementary Data

Supplementary Data associated with this article are available in the electronic form at http://nopr.niscair.res.in/jinfo/ijca/IJCA_60A(12)1551-1556_SupplData.pdf.

References

1 Kansara M, Teng M W, Smyth M J & Thomas D M, *Nat Rev Cancer*, 14 (2014) 722.
2 Corre I, Verrecchia F, Crenn V, Redini F & Trichet V, *Cells*, 9 (2020) Article 976.
3 Kager L, Tamamyan G & Bielack S, *Future Oncol*, 13 (2017) 357.
4 Kumari B, Adhikari S, Matalobos J S & Das D, *J Mol Struct*, 1151 (2018) 169.
5 Hu M L, Razavi S A A, Piroozzadeh M & Morsali A, *Inorg Chem Front*, 7 (2020) 1598.
6 Hu M L, Mohammad Y M & Morsali A, *Coord Chem Rev*, 387 (2019) 415.

7 Fan L, Zhao D, Li B, Wang F, Deng Y, Peng Y, Wang X & Zhang X, *Spectrochim Acta A*, 264 (2022) Article 120232.
8 Fan L, Zhao D, Zhang H, Wang F, Li B, Yang L, Deng Y & Zhang X, *Micropor Mesopor Mater,* 326 (2021) 111396.
9 Li R F, Liu X F, Zhang T, Zhang X Y & Feng X, *J Mol Struct*, 1075 (2014) 456.
10 Li R F, Gu Y X, Liu X F, Feng X & Ma L F, *Z Anorg Allg Chem*, 641 (2015) 1114.
11 Lavrenova L G, Kuz'menko T A, Ivanova A D, Smolentsev A I, Komarov V Y, Bogomyakov A S, Sheludyakova L A & Vorontsova E V, *New J Chem*, 41 (2017) 4341.
12 Prosser K E, Chang S W, Saraci F, Le P H & Walsby C J, *J Inorg Biochem*, 167 (2017) 89.
13 Hu J, Guo Y, Zhao J & Zhang J, *Bioorg Med Chem*, 25 (2017) 5733.
14 Wu H, Yuan J, Bai Y, Pan G, Wang H, Kong J, Fan X & Liu H, *Dalton Trans*, 41 (2012) 8829.
15 Pal S, Hwang W S, Lin I J B & Lee C S, *J Mol Catal A: Chem*, 269 (2007) 197.
16 Shankar B, Hussain F & Sathiyendiran M, *J Organomet Chem*, 719 (2012) 26.
17 Liu Q D, Jia W L & Wang S, *Inorg Chem*, 44 (2005) 1332.
18 Aschner M, Guilarte T R, Schneider J S & Zheng W, *Toxicol Appl Pharmacol*, 221 (2007) 131.
19 Calzolari A, Oliviero I, Deaglio S, Mariani G, Biffoni M, Sposi N M, Malavasi F, Peschie C & Testa U, *Blood Cells Mol Dis*, 39 (2007) 82.
20 Ansari K I, Grant J D, Kasiri S, Woldemariam G, Shrestha B & Mamdal S S, *J Inorg Biochem*, 103 (2009) 818.
21 Zhou D F, Chen Q Y, Qi Y, Fu H J, Li Z, Zhao K D & Gao J, *Inorg Chem*, 50 (2011) 6929.
22 Cui L S, Gan Y L, Li Y C & Meng J R, *J Mol Struct*, 1147 (2017) 317.
23 Wang H, Han S, Wang J, Dun L, Zhang B, Chen X, Li W & Li C, *J Mol Struct*, 1204 (2020) Article 127466.